METASTABLE DYNAMICS AND EXPONENTIAL ASYMPTOTICS IN MULTI-DIMENSIONAL DOMAINS

Michael J. Ward[1]
Department of Mathematics, University of British Columbia
Vancouver, B.C. V6T 1Z2, Canada

Abstract

Certain singularly perturbed partial differential equations exhibit a phenomenon known as dynamic metastability, whereby the solution evolves on an asymptotically exponentially long time interval as the singular perturbation parameter ϵ tends to zero. This article illustrates a technique to analyze metastable behavior for a range of problems in multi-dimensional domains. The problems considered include the exit problem for diffusion in a potential well, models of interface propagation in materials science, an activator-inhibitor model in mathematical biology, and a flame-front problem. Many of these problems can be formulated in terms of non-local partial differential equations. This non-local feature is shown to be essential to the existence of metastable behavior.

1 Introduction

Certain time-dependent singularly perturbed partial differential equations exhibit a phenomenon known as dynamic metastability, whereby the solution evolves on an asymptotically exponentially long time interval as the singular perturbation parameter ϵ tends to zero. Metastable dynamics has been observed and analyzed over the past decade for certain classes of problems in a *one-spatial* dimensional setting (eg. [1], [8], [10], [12], [22], [31], [32], [40]). In this article we give examples of various problems that exhibit metastable dynamics in *multi-spatial* dimensional domains and we outline an asymptotic technique, known as the projection method, to analyze the metastable dynamics. The problems considered include the exit problem for diffusion in a potential well, models of interface propagation in materials science, an activator-inhibitor model in mathematical biology, and a flame-front problem.

There are several common features to many of these problems. The first common feature is that in the limit $\epsilon \to 0$, each problem admits an asymptotic quasi-equilibrium solution $u_q(\mathbf{x}, \epsilon; \alpha)$, in terms of some unknown parameter vector $\alpha \in S$, where S is some parameter set. This quasi-equilibrium solution satisfies the equilibrium problem up to exponentially small terms as $\epsilon \to 0$. The

[1]This work was supported by NSERC grant 5-81541

associated linearization of the nonlinear problem around u_q is exponentially ill-conditioned as $\epsilon \to 0$ for $\alpha \in S$. For some of the nonlinear problems considered below, this ill-conditioning is a consequence of an exponential localization of a radially symmetric canonical solution combined with a near translation invariance. In this situation and in an N-dimensional domain D, α is an N-vector giving the coordinates of the center $\mathbf{x_0}$ of the localized structure in D. As a result of the exponential ill-conditioning, exponential asymptotics is required to calculate the correct value of α corresponding to a true asymptotic equilibrium solution. In addition, metastable dynamics of the canonical solution for the time-dependent problem will occur when the exponentially small eigenvalues are the principal eigenvalues associated with the linearization. This metastable dynamics is then given by $u \sim u_q\left(\mathbf{x}, \epsilon\,; \alpha(t;\epsilon)\right)$, where $\alpha(t;\epsilon)$ satisfies a finite dimensional dynamical system. This dynamical system evolves on an exponentially slow time scale as $\epsilon \to 0$.

A critical common feature in many of the problems considered here, which allows for the existence of metastable dynamics in a multi-spatial dimensional setting, is a non-local or global condition, such as mass conservation. This non-local condition, which arises in a natural way for the problems considered below, is essential for ensuring that the exponentially small eigenvalues are the *principal* eigenvalues associated with the linearization. This allows us to seek a quasi-steady solution to the nonlinear problem in the form $u \sim u_q(\mathbf{x}, \epsilon\,; \alpha(t;\epsilon))$. Since the principal eigenvalues associated with the linearized problem are exponentially small, the solution to this quasi-steady linearization must satisfy limiting solvability conditions as $\epsilon \to 0$ that ensures that the 'residual" is orthogonal to the eigenspace associated with the exponentially small eigenvalues. From this projection step and from certain key asymptotic exponential estimates for eigenfunctions on the boundary of the domain, an explicit asymptotic differential equation for $\alpha(t;\epsilon)$, characterizing the metastable dynamics, is derived. For all the problems considered below, the dynamics of $\alpha(t;\epsilon)$ is reduced to a surface integral over the boundary of the domain D. An asymptotic evaluation of this integral shows that only certain special points on the boundary of D influence the metastable dynamics.

The outline of this paper is as follows. In §2, we consider the linear exit time problem for diffusion in a potential well modeled by a well-known singularly perturbed convection-diffusion equation (i. e. [27]). When the potential is radially symmetric, it is shown that the metastable dynamics are influenced very strongly by the points on the boundary of the domain that are closest to the minimum of the potential. In §3, we analyze the motion of a straight-line interface for the Allen-Cahn equation in the neck, or channel, region of a two-dimensional dumbbell-shaped domain as shown in Fig. 1 below. The motion of such an interface is metastable and depends very strongly on the local behavior of the boundary of the domain near the connection points between the channel and the two lobes of the dumbbell (see [6], [19], [35]). In §4 we illustrate the metastable dynamics of bubble solutions for the constrained Allen-Cahn equa-

tion, which conserves mass and has applications to material science. In §5 we analyze metastable spike dynamics for an activator-inhibitor model in the limit of large inhibitor diffusivity, which yields the shadow problem (see [29]). The problems in §4 and §5 are both non-local and involve radially symmetric canonical solutions u_q whose center $\alpha = \mathbf{x_0}(t)$ drifts exponentially slowly towards the nearest point on the boundary of the domain. Finally, in §6 we briefly describe a flame-front model exhibiting metastable dynamics.

2 Metastable Dynamics for the Exit Problem

The following linear convection-diffusion equation arises in determining the exit time distribution for a Brownian particle confined by a potential well $\Psi(\mathbf{x})$ ([24], [25], [27]):

$$u_t = \epsilon \triangle u - \nabla\Psi \cdot \nabla u\,, \quad \mathbf{x} \in D\,, \quad t > 0\,, \tag{1a}$$

$$u = u_b(\mathbf{x})\,, \quad \mathbf{x} \in \partial D\,; \qquad u(\mathbf{x},0) = u_0(\mathbf{x})\,, \tag{1b}$$

where $\mathbf{x} = (x_1, x_2)$, $u = u(\mathbf{x}, t)$, $\epsilon \to 0$, D is a bounded two-dimensional domain, and $u_b(\mathbf{x})$ and $u_0(\mathbf{x})$ are smooth. Let $\bar{D} = D \cup \partial D$. It is assumed that the potential $\Psi(\mathbf{x})$ has a unique global minimum on $\bar{D}$ at some interior point $\mathbf{x_0} \in D$, where

$$\Psi(\mathbf{x_0}) = 0\,, \qquad \nabla\Psi(\mathbf{x_0}) = 0\,, \qquad H\left[\Psi(\mathbf{x_0})\right] > 0\,. \tag{2}$$

Here $H(\Psi) \equiv \Psi_{x_1x_1}\Psi_{x_2x_2} - \Psi^2_{x_1x_2}$ is the Hessian. We also assume that $\nabla\Psi(\mathbf{x}) \neq 0$ for $\mathbf{x} \neq \mathbf{x_0}$ and that $\nabla\Psi \cdot \hat{n} > 0$ on ∂D, where $\hat{n}$ is the unit outward normal to ∂D. As shown in [38], this problem provides the simplest example of metastable behavior in a multi-dimensional setting. Below we sketch the outline of the metastability analysis given in [38].

The following eigenvalue problem associated with (1a)-(1b) is central to the analysis:

$$L_\epsilon\phi \equiv \epsilon\triangle\phi - \nabla\Psi\cdot\nabla\phi = -\lambda\phi\,, \quad \mathbf{x} \in D\,; \quad \phi = 0\,, \quad \mathbf{x} \in \partial D\,, \tag{3a}$$

$$(\phi,\phi)_w \equiv \int_D \phi^2 w\, dx = 1\,, \qquad w \equiv e^{-\Psi/\epsilon}\,. \tag{3b}$$

The eigenvalues λ_j for $j \geq 0$ are real with $\lambda_j > 0$ and $(\phi_j, \phi_k)_w = \delta_{jk}$ for $j, k = 0, 1, \ldots$ Suppose that the minimum value of Ψ on ∂D is taken at N distinct points $\mathbf{y_j} \in \partial D$ for $j = 1, .., N$, and that these minima are non-degenerate. Then, as is shown in [27], the principal eigenvalue λ_0 of (3a) is exponentially small as $\epsilon \to 0$ and has the asymptotic estimate

$$\lambda_0 \sim (2\pi\epsilon)^{-1/2}\left(H\left[\Psi(\mathbf{x_0})\right]\right)^{1/2} e^{-\Psi^*/\epsilon} \sum_{j=1}^{N} |\nabla\Psi(\mathbf{y_j})| r_j^{-1/2}\,. \tag{4}$$

Here $\Psi^* \equiv \Psi(\mathbf{y_j})$ for $j = 1, .., N$, and

$$r_j \equiv |\nabla\Psi|^{-2} \left[\Psi_{x_1x_1}\Psi_{x_2}^2 - 2\Psi_{x_1x_2}\Psi_{x_1}\Psi_{x_2} + \Psi_{x_2x_2}\Psi_{x_1}^2 + \kappa_j|\nabla\Psi|^3\right]\Big|_{\mathbf{x}=\mathbf{y_j}}, \quad (5)$$

where $\kappa_j < 0$ is the curvature of ∂D at $\mathbf{y_j}$.

The reciprocal of λ_0 determines the expected time for a particle initially located at $\mathbf{x} = \mathbf{x_0}$ to leave D. The most likely points of exit of the particle are those that minimize Ψ on D. Therefore, if Ψ is radially symmetric about $\mathbf{x_0}$, the asymptotic estimate for λ_0 depends critically on certain local information near the points on the boundary that are closest to ∂D. This feature will also occur for all of the problems considered in the sections below.

In terms of a normalization constant M_0, the corresponding eigenfunction ϕ_0 has the boundary layer form

$$\phi_0 \sim M_0\left(1 - e^{\gamma\eta/\epsilon}\right), \qquad \text{for} \qquad \gamma = \gamma(s) \equiv \nabla\Psi\cdot\hat{n}\Big|_{\partial D} > 0\,. \quad (6)$$

Here s denotes arclength along ∂D and $-\eta$ is the distance from $\mathbf{x} \in D$ to ∂D. Since $\gamma > 0$, $\phi_0 \to M_0$ as $\eta/\epsilon \to -\infty$.

For $\epsilon \to 0$, the equilibrium solution $U(\mathbf{x};\epsilon)$ to (1) is a constant away from ∂D and has a boundary layer form near ∂D. It is given to leading order by

$$U(\mathbf{x};\epsilon) \sim \tilde{u}^{\epsilon}\left[\mathbf{x}; A_{0e}\right] \equiv A_{0e} + (u_b(s) - A_{0e})\, e^{\gamma\eta/\epsilon}\,, \quad (7)$$

for some undetermined constant A_{0e}. Here u_b is written in terms of the arclength s. The determination of A_{0e} requires exponential precision as a result of the exponential ill-conditioning of the operator as is evident from (4). For the time-dependent problem when $t \gg 1$, we look for a solution of the form $u(\mathbf{x},t) \sim \tilde{u}^{\epsilon}\left[\mathbf{x}; A_0(t)\right]$, where $A_0(t)$ is a function to be determined. As a result of the exponentially small principal eigenvalue λ_0, the function $A_0(t)$ approaches its equilibrium value A_{0e} only over an asymptotically exponentially long time interval as $\epsilon \to 0$. This exponentially slow relaxation to the equilibrium value is known as metastable dynamics.

A projection method, which is based on a limiting solvability condition, can be used to calculate an explicit ODE for $A_0(t)$ characterizing the metastable behavior (see [38]). To do so, we introduce a correction $v(\mathbf{x},t)$ by $u(\mathbf{x},t) = \tilde{u}^{\epsilon}\left[\mathbf{x}; A_0(t)\right] + v(\mathbf{x},t)$. Substituting in (1), we obtain that $v(\mathbf{x},t)$ satisfies

$$v_t = L_\epsilon v - \tilde{u}_t^{\epsilon} + L_\epsilon\tilde{u}^{\epsilon}\,, \quad \mathbf{x} \in D\,, \quad t > 0\,, \quad (8a)$$

$$v = u_b - \tilde{u}^{\epsilon}\,, \ \mathbf{x} \in \partial D\,, \quad (8b)$$

$$v(\mathbf{x},0) = u_0(\mathbf{x}) - \tilde{u}^{\epsilon}\left[\mathbf{x}; A_0(0)\right]\,, \ \mathbf{x} \in D\,. \quad (8c)$$

We then expand v in terms of the eigenfunctions ϕ_j of (3) as

$$v(\mathbf{x},t) = \sum_{j=0}^{\infty} c_j(t)\phi_j(\mathbf{x})\,, \quad (9)$$

where the coefficient $c_j(t)$ satisfies

$$c_j^{'} + \lambda_j c_j = \left(\phi_j, L_\epsilon \tilde{u}^\epsilon\right)_w - \int_{\partial D} \epsilon w v \, \partial_n \phi_j \, ds - \left(\phi_j, \tilde{u}_t^\epsilon\right)_w \, , \tag{10}$$

together with the initial value

$$c_j(0) = \int_D \left(u_0(\mathbf{x}) - \tilde{u}^\epsilon \left[\mathbf{x}; A_0(0)\right]\right) \, \phi_j w \, dx \, . \tag{11}$$

Here $w \equiv e^{-\Psi/\epsilon}$, and, in (10), ∂_n denotes the outward normal derivative to ∂D.

We now impose the limiting solvability condition. To ensure that $v \ll \tilde{u}^\epsilon$ over exponentially long time intervals it is necessary that $c_0(t) \equiv 0$. Hence, (10) gives an ODE for $A_0(t)$ and (11) yields the initial value $A_0(0)$. Since w is exponentially localized and ϕ_0 is known asymptotically, the various terms in (10) and (11) can be estimated asymptotically as in [38] to obtain the following explicit ordinary differential equation for $A_0(t)$:

$$A_0^{'} \sim -\lambda_0 A_0 + \beta e^{-\Psi^*/\epsilon} \sum_{j=1}^{N} u_b(\mathbf{y_j}) |\nabla \Psi(\mathbf{y_j})| r_j^{-1/2} \, , \qquad A_0(0) \sim u_0(\mathbf{x}_0) \, . \tag{12}$$

Here, λ_0 is given in (4), r_j is defined in (5), $\mathbf{x}_0$ is the global minimum of Ψ in $\bar{D}$, and $\beta \equiv \left(H[\Psi(\mathbf{x}_0)]/(2\pi\epsilon)\right)^{1/2}$, where H is the Hessian. Moreover, $\mathbf{y_j} \in \partial D$, for $j = 1, .., N$, are those points where Ψ is minimized on ∂D (with a non-degenerate minimum) with minimum value $\Psi^* \equiv \Psi(\mathbf{y_j})$ for $j = 1, .., N$.

In summary, the metastable dynamics for (1) for $t \gg 1$, is given by $u(\mathbf{x}, t) \sim \tilde{u}^\epsilon \left[\mathbf{x}; A_0(t)\right]$, where $\tilde{u}^\epsilon$ is defined in (7) and $A_0(t)$ satisfies (12). As $t \to \infty$, $A_0(t) \to A_{0e}$, where A_{0e} is the weighted average over the minimum points $\mathbf{y_j}$ of Ψ on ∂D

$$A_{0e} = \sum_{j=1}^{N} u_b(\mathbf{y_j}) \frac{|\nabla \Psi(\mathbf{y_j})|}{r_j^{1/2}} \left(\sum_{j=1}^{N} \frac{|\nabla \Psi(\mathbf{y_j})|}{r_j^{1/2}} \right)^{-1} \tag{13}$$

This result for A_{0e} is given in [27].

2.1 An Explicit Example

To illustrate this result, we consider a simple specific example. Let D denote the interior of the ellipse $x_2^2 + x_1^2/4 \leq 1$ and take $u_b = -x_2 + x_2^2/2$ as the boundary data on ∂D. Let $\Psi = x_1^2 + x_2^2$. Then, it is clear that $\mathbf{x}_0 = (0, 0)$, $N = 2$, and $\mathbf{y_1} = (0, 1)$, $\mathbf{y_2} = (0, -1)$. A simple calculation shows that $H\left[\psi(\mathbf{x}_0)\right] = 4$, $\Psi^* = 1$, and $r_j = 8/(14\pi)^{1/2}$ for $j = 1, 2$. Thus, we obtain from (12) that

$$A_0^{'} \sim \left(\frac{8}{14\pi\epsilon}\right)^{1/2} e^{-1/\epsilon} \left(1 - 2A_0\right) \, . \tag{14}$$

Thus, away from the boundary layer near ∂D and for t sufficiently large, we have that the outer limit of $u(\mathbf{x},t)$ satisfies

$$u(\mathbf{x},t) \sim A_0(t) = \frac{1}{2} + \left(A_0(0) - \frac{1}{2}\right) e^{-\nu t}\,, \qquad \nu \equiv 2\left(\frac{8}{14\pi\epsilon}\right)^{1/2} e^{-1/\epsilon}\,. \quad (15)$$

3 A Bistable Nonlinearity in a Dumbbell-Shaped Domain

The simplest model for the phase separation of a binary mixture is the Allen-Cahn equation

$$u_t = \epsilon^2 \Delta u + Q(u)\,, \qquad \mathbf{x} \in D \subset \mathbf{R^2}\,, \quad (16a)$$

$$\partial_n u = 0\,, \qquad \mathbf{x} \in \partial D\,. \quad (16b)$$

Here $\epsilon \ll 1$ and $Q(u)$ is a bistable nonlinearity having three zeroes located at $u = s_- < 0$, $u = 0$, and $u = s_+ > 0$, with

$$Q(s_\pm) < 0\,, \quad Q(0) > 0\,, \quad V(s_+) = 0\,, \quad V(u) = -\int_{s_-}^{u} Q(\eta)\, d\eta\,. \quad (17)$$

Thus, $V(u)$ is a double-well potential with wells of equal depth at s_+ and s_-. The two-dimensional dumbbell-shaped domain D is taken to be of the form $D = R \cup D_- \cup D_+$ where R is the rectangle $[0,1] \times [0,b]$, and D_- and D_+ are the two attachments on its sides (see Fig. 1)

Starting from initial data, the solution to (16) quickly develops internal layers of width $O(\epsilon)$ that separate the two minima s_+ and s_- of the potential $V(u)$. The normal velocity v of such an interface is well-known to be $v \sim \epsilon^2 \kappa$, where κ is the curvature of the interface (see [34]). In addition, if the interface intersects the boundary ∂D, it must do so orthogonally.

In this section, we will investigate the dynamics of (16) when the interface is initially the straight line segment $x = x_0$, with $0 < x_0 < 1$, that connects the two sides of R as shown in Fig. 1. In this case, $\kappa = 0$ and the velocity curvature law $v \sim \epsilon^2 \kappa$ gives no information about the motion of the interface.

In this situation, the dynamics of the interface depends critically on the nature of the boundary of the domain at the corner points of R given by $(0,0)$, $(0,b)$, $(1,0)$, and $(1,b)$. It is assumed that the domain boundary is smooth and that near these corners points, ∂D has the local behavior $\partial D = \{(x,y)\,|\,y = \psi_i(x)\}$ where

$$\text{near } (0,0)\,; \quad y = \psi_1(x), \qquad \psi_1'(x) \sim -K_1(-x)^{\alpha_1}, \ \text{as } x \to 0^-, \quad (18a)$$

$$\text{near } (0,b)\,; \quad y = \psi_2(x) + b, \qquad \psi_2'(x) \sim K_2(-x)^{\alpha_2}, \ \text{as } x \to 0^-, \quad (18b)$$

$$\text{near } (1,0)\,; \quad y = \psi_3(x), \qquad \psi_3'(x) \sim K_3(x-1)^{\alpha_3}, \ \text{as } x \to 1^+, \quad (18c)$$

$$\text{near } (1,b)\,; \quad y = \psi_4(x) + b, \qquad \psi_4'(x) \sim -K_4(x-1)^{\alpha_4}, \ \text{as } x \to 1^+. \quad (18d)$$

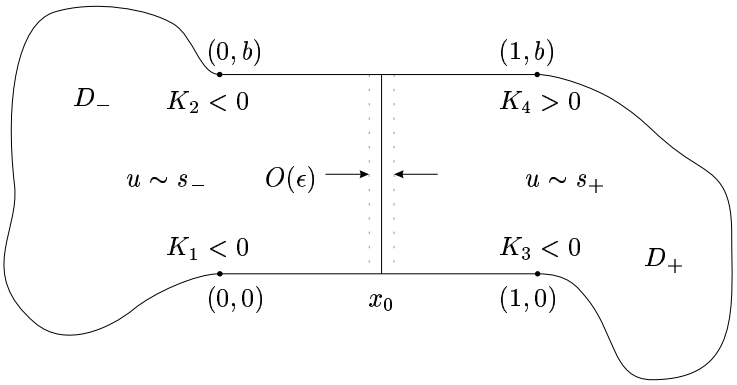

Figure 1: A dumbbell-shaped domain D and an interface centered at x_0.

Here $\alpha_i > 0$, for each i, and the constant K_i is proportional to the curvature of the i^{th} corner when $\alpha_i = 1$.

Since the straight-line internal layer solution decays exponentially for $|x - x_0| \gg O(\epsilon)$, exponential precision is required to determine the motion of the interface. The projection method was used in [35] to incorporate such exponentially small effects and to calculate metastable dynamics. The key steps of the method are as follows: First an equilibrium solution to (16) in R is constructed. Next, the spectral properties of the linearization of (16) around the equilibrium solution are analyzed asymptotically to show the existence of an exponentially small principal eigenvalue, which is responsible for the metastable behavior. Finally, a limiting solvability condition of Fredholm type is used to derive an explicit ODE for the interface location in the straight channel R. Below we summarize the results of the analysis of [36].

We first construct an equilibrium solution. In the limit $\epsilon \to 0$, the straight-line equilibrium internal layer solution for (16) depends only on x and is given by $u(x;\epsilon) = u_0\left[\epsilon^{-1}(x - x_0)\right]$, where x_0 is the center of the layer with $0 < x_0 < 1$, and $u_0(z)$ satisfies

$$u_0'' + Q(u_0) = 0, \quad -\infty < z < \infty, \tag{19a}$$

$$u_0(0) = 0; \quad u_0(z) \sim s_\pm, \ \text{as } z \to \pm\infty. \tag{19b}$$

The far-field behavior of $u_0(z)$ is given by

$$u_0(z) \sim \begin{cases} s_+ - a_+ e^{-\nu_+ z}, & z \to +\infty\,, \\ s_- + a_- e^{\nu_- z}, & z \to -\infty\,. \end{cases} \tag{20}$$

Here the positive constants $\nu_\pm$ and $a_\pm$ are defined by

$$\nu_\pm = \left[-Q'(s_\pm)\right]^{1/2}, \tag{21}$$

$$\log a_\pm = \log(\pm s_\pm) + \int_0^{s_\pm} \left(\frac{\pm \nu_\pm}{[2V(\eta)]^{1/2}} + \frac{1}{\eta - s_\pm} \right) d\eta \,. \tag{22}$$

The eigenvalue problem associated with linearizing (16) about $u_0[\epsilon^{-1}(x-x_0)]$ is

$$L_\epsilon \phi \equiv \epsilon^2 \Delta \phi + Q'(u_0)\phi = \lambda \phi \,, \qquad \mathbf{x} \in D \,, \tag{23a}$$

$$\partial_n \phi = 0 \,, \qquad \mathbf{x} \in \partial D \,, \tag{23b}$$

$$(\phi, \phi) = \int_D \phi^2 \, d\mathbf{x} = 1 \,. \tag{23c}$$

Here $(u,v) \equiv \int_D uv \, d\mathbf{x}$. The eigenpairs are labeled by λ_j, ϕ_j respectively for $j = 0, 1, \ldots$, with $\lambda_j \to -\infty$ as $j \to \infty$.

We assume that the distance from the interface to the corners of R is $O(1)$. To estimate the principal eigenpair, we notice that $L_\epsilon u_0'[\epsilon^{-1}(x-x_0)] = 0$, that u_0' has no nodal lines, and that u_0' fails to satisfy the boundary condition (23b) by only exponentially small terms. Thus, as shown in [35], the principal eigenfunction ϕ_0 has the form $\phi_0 \sim N_0 \, [u_0' + \phi_{L_0}]$, where N_0 is a normalization constant and ϕ_{L_0} is a boundary layer function localized near the curved parts of ∂D that is used to satisfy the boundary condition (23b). Then, Green's identity can be applied to (23a) and u_0' to yield

$$\lambda_0 (u_0', \phi_0) = -\epsilon^2 \int_{\partial D} \phi_0 \partial_n u_0' \, ds \,. \tag{24}$$

After calculating ϕ_0 on ∂D, this equation is used to calculate the exponentially small eigenvalue λ_0. An important observation is that $\partial_n u_0' = 0$ except along the two attachments D_+ and D_-. Hence, the surface integral on the right side of (24) vanishes identically over R. In addition, since u_0' and ϕ_0 are both exponentially decaying away from the internal layer region it is clear that this surface integral is dominated asymptotically by the contribution arising from the corner regions of the attachments D_+ and D_-.

The boundary layer correction ϕ_{L_0} is calculated in [35] using a local coordinate system defined near ∂D. This allows us to obtain the following expression for ϕ_0 on ∂D as needed in (24):

$$\phi_0 \sim \begin{cases} N_0 a_- \nu_- e^{\nu_- \epsilon^{-1}(x-x_0)} \, (1 - \nu_- n_x) & x < x_0 \,, \\ N_0 a_+ \nu_+ e^{-\nu_+ \epsilon^{-1}(x-x_0)} \, (1 + \nu_+ n_x) & x > x_0 \,. \end{cases} \tag{25}$$

Here $\hat{\mathbf{n}} = (n_x, n_y)$ is the outward unit normal vector to ∂D. The dominant contribution to the inner product on the left side of (24) arises from the region near $x = x_0$ and is given asymptotically by

$$(u_0', \phi_0) \sim \epsilon N_0 b \beta \,, \qquad \text{where} \qquad \beta \equiv \int_{-\infty}^{\infty} [u_0'(z)]^2 \, dz \,. \tag{26}$$

Substituting (26), (25) and (20) into (24) we get the following expression for λ_0

$$\lambda_0 \sim -\frac{1}{b\beta}\left\{\int_{\partial D_-} a_-^2\nu_-^3 e^{2\nu_-\epsilon^{-1}(x-x_0)}(1-\nu_- n_x)n_x\,ds - \int_{\partial D_+} a_+^2\nu_+^3 e^{-2\nu_+\epsilon^{-1}(x-x_0)}(1+\nu_+ n_x)n_x\,ds\right\}. \tag{27}$$

The dominant contribution to the two surface integrals above arises from the corner regions. In these regions, we can use (18) to calculate n_x in terms of K_i and α_i and then we apply Laplace's method. In this way, we obtain in [35] the following explicit asymptotic formula for the principal eigenvalue λ_0 as $\epsilon \to 0$:

$$\lambda_0 \sim \frac{1}{b\beta}\left\{a_-^2\nu_-^3 A_- e^{-2\nu_-\epsilon^{-1}x_0} + a_+^2\nu_+^3 A_+ e^{-2\nu_+\epsilon^{-1}(1-x_0)}\right\}. \tag{28}$$

Here $A_\pm$ are defined by

$$A_- = K_1\left(\frac{\epsilon}{2\nu_-}\right)^{\alpha_1+1}\Gamma(\alpha_1+1) + K_2\left(\frac{\epsilon}{2\nu_-}\right)^{\alpha_2+1}\Gamma(\alpha_2+1), \tag{29a}$$

$$A_+ = K_3\left(\frac{\epsilon}{2\nu_+}\right)^{\alpha_3+1}\Gamma(\alpha_3+1) + K_4\left(\frac{\epsilon}{2\nu_+}\right)^{\alpha_4+1}\Gamma(\alpha_4+1), \tag{29b}$$

and $\Gamma(z)$ denotes the Gamma function.

Next the projection method is used to determine an ODE for the interface location $x_0 = x_0(t)$ for (16) in the rectangle R. It is assumed that the initial data has the special form $u_0[\epsilon^{-1}(x-x_0^0)]$, so that $x_0(0) = x_0^0$. Introduce the correction w by

$$u(\mathbf{x},t) = u_0[\epsilon^{-1}(x - x_0(t))] + w(\mathbf{x},t), \tag{30}$$

where $\mathbf{x} = (x,y)$ and where we assume that $w \ll u_0$ and $w_t \ll \partial_t u_0$ uniformly in time. This yields the quasi-steady linearization of (16) about u_0

$$L_\epsilon w \equiv \epsilon^2\Delta w + Q'(u_0)w = \partial_t u_0, \qquad \mathbf{x}\in D, \tag{31a}$$

$$\partial_n w = -\partial_n u_0, \qquad \mathbf{x}\in\partial D. \tag{31b}$$

The solution to (31) is then expanded in terms of the eigenfunctions of (23) as $w = \sum_{j=0}^{\infty} c_j\phi_j/\lambda_j$, where the c_j are given by

$$c_j = (\phi_j, \partial_t u_0) + \epsilon^2\int_{\partial D}\phi_j\partial_n u_0\,ds. \tag{32}$$

Since λ_0, as estimated in (28), is exponentially small as $\epsilon\to 0$, we require that $c_0 \to 0$ as $\epsilon\to 0$ in order to ensure that $w \ll u_0$ over exponentially long time intervals. This limiting solvability yields the ODE for $x_0(t)$

$$(\phi_0, \partial_t u_0) = -\epsilon^2\int_{\partial D}\phi_0\partial_n u_0\,ds. \tag{33}$$

Finally, the terms in (33) are evaluated asymptotically as $\epsilon \to 0$ as in [35] to give the following explicit ordinary differential equation for $x_0(t)$:

$$x_0'(t) \sim \frac{\epsilon}{b\beta}\left\{a_+^2\nu_+^2 A_+ e^{-2\nu_+\epsilon^{-1}(1-x_0)} - a_-^2\nu_-^2 A_- e^{-2\nu_-\epsilon^{-1}x_0}\right\} . \qquad (34)$$

Here, b is the width of R, $\nu_\pm$ and $a_\pm$ are defined in (21) and (22), β is defined in (26), and $A_\pm$ is defined in (29).

Thus, the motion of the interface is determined by the local behavior at the corners of R and by the distance from the interface to these corners. The interface will move according to (34) until a steady state is attained or until the interface has moved to one of the sides of R. In the latter case, the subsequent evolution of the interface after it enters one of the attachements is given by the usual velocity-curvature law. The result (34) agrees with that obtained in [6] and [19] using a different method.

3.1 Some Explicit Examples

When $A_+A_- > 0$, we see from (34) that there is a unique equilibrium interface location given by

$$x_0^e \sim \frac{\nu_+}{\nu_+ + \nu_-} + \frac{\epsilon}{2(\nu_+ + \nu_-)}\log\left(\frac{a_-^2\nu_-^2 A_-}{a_+^2\nu_+^2 A_+}\right) . \qquad (35)$$

A sufficient condition for this equilibrium solution to be stable is that $K_i < 0$ for $i = 1, .., 4$, which corresponds to a domain that is non-convex near each of the corners. This yields an example of a stable non-constant equilibrium solution in a non-convex domain. Such an equilibrium solution is impossible when the domain is convex (see [26]). A sufficient condition for the equilibrium solution to be unstable is that $K_i > 0$ for $i = 1, \ldots, 4$. This corresponds to a domain that is convex near each corner. When $A_+A_- < 0$ there is no equilibrium solution.

We conclude by giving an example of the slow dynamics. Let $Q(u) = 2(u - u^3)$, for which we get from (19) that $u_0(z) = \tanh z$. Then, we calculate $a_\pm = 2$, $\nu_\pm = 2$, $s_\pm = \pm 1$ and $\beta = 4/3$. Suppose that $\alpha_i = \alpha > 0$ for each i. Then, the ODE (34), becomes

$$x_0' \sim \frac{12\epsilon^{\alpha+2}\Gamma(\alpha+1)}{b4^{\alpha+1}}\left[(K_3+K_4)e^{-4\epsilon^{-1}(1-x_0)} - (K_1+K_2)e^{-4\epsilon^{-1}x_0}\right] , \qquad (36)$$

which has the steady-state location

$$x_0^e \sim \frac{1}{2} + \frac{\epsilon}{8}\log\left(\frac{K_1+K_2}{K_3+K_4}\right) . \qquad (37)$$

If $K_i < 0$ for $i = 1, \ldots, 4$, then this steady state is stable. Alternatively, if $K_i > 0$ for $i = 1, \ldots, 4$, then the steady state is unstable.

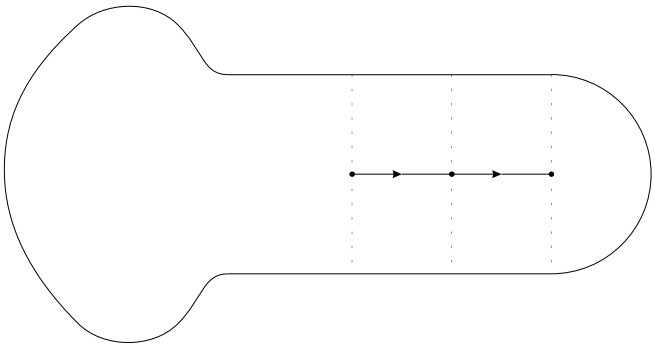

Figure 2: Since K_1, $K_2 < 0$ and K_3, $K_4 > 0$ for this domain, the interface moves to the right.

Notice that when K_1, $K_2 < 0$ and K_3, $K_4 > 0$, then from (36), $x_0' > 0$ for all time. In this case, the interface location, x_0 will move monotonically but exponentially slowly towards $x = 1$ (see Fig. 2). Once the interface reaches $x = 1$, it will move in the attachment D_+ by the velocity curvature law until it collapses against the boundary of D_+. Similarly, when K_1, $K_2 > 0$ and K_3, $K_4 < 0$, we have $x_0' < 0$ and the interface location will monotonically $x = 0$.

4 The Constrained Allen-Cahn Equation

A simple model for the phase separation of a binary mixture is the Allen-Cahn equation with a mass constraint as introduced in [33],

$$u_t = \epsilon^2 \Delta u + Q(u) - \sigma\,, \qquad \mathbf{x} \in D \subset \mathbf{R^2}\,, \tag{38a}$$

$$\partial_n u = 0\,, \qquad \mathbf{x} \in \partial D\,, \tag{38b}$$

$$\int_D u(\mathbf{x}, t)\, d\mathbf{x} = M\,. \tag{38c}$$

Here $u = u(\mathbf{x}, t)$ is the concentration of one of the two species, $\mathbf{x} = (x, y)$, $\epsilon \ll 1$, D is a bounded two-dimensional domain, and the mass M is constant. We assume that $Q(u) = -V'(u)$, where $V(u)$ is a double-well potential with minima at $u = s_\pm$ where $V(s_\pm) = 0$. The function $Q(u)$ satisfies (17). The problem (38) is a non-local reaction-diffusion equation since, in order to satisfy the mass constraint (38c), we require

$$\sigma = \frac{1}{|D|} \int_D Q(u)\, d\mathbf{x}\,. \tag{39}$$

Here $|D|$ is the total area of D.

We now describe the different stages of the dynamics for (38) that have been studied in detail in [2], [3], [4], [5], [33], [36] and [41]. The various stages of the dynamics of a single closed interface for (38) are shown qualitatively in Fig. 3.

The first stage is a transient phase. Starting from arbitrary initial data, in an $O(1)$ time interval the solution to (38) develops internal layers of width $O(\epsilon)$ separating the two minina of the potential well. Then, as shown by the asymptotic analysis of [33], for $\epsilon \to 0$ the normal velocity v of a single closed interface Γ satisfies the constrained velocity-curvature law

$$v \sim \epsilon^2 \left(\kappa - \frac{1}{|\Gamma|} \int_\Gamma \kappa \, ds \right) . \tag{40}$$

Here κ is the curvature of Γ. This expression holds for interfaces in the interior of D and for interfaces that are connected to ∂D orthogonally. As shown in [13], a single closed convex interface evolving according to (40) will tend to a circle that encloses the same area.

The law of motion (40) gives no indication of the nature of the motion of a single circular interface contained in D. Such an interface is also referred to as a *bubble*. As shown in [2], [4], [5], and [41], the motion of such a bubble is metastable. The key feature that leads to this metastable behavior is the conservation of mass condition. As shown in [41], a bubble solution to (38) drifts exponentially slowly, without change of shape, towards the closest point on ∂D. This slow drift is due to an exponentially weak interaction between the tail of the bubble solution and the boundary ∂D. It was derived in [41] that the distance $r_m(t)$ between the center of the bubble and the closest point on the boundary of D, satisfies the asymptotic ODE

$$r_m'(t) \sim -\frac{\epsilon^{3/2} \zeta r_m^{-1/2}}{(1-\kappa_m r_m)^{1/2}} e^{-2\nu_+^\epsilon \epsilon^{-1}(r_m - r_b)} . \tag{41}$$

Here κ_m is the curvature of ∂D at the point closest to the bubble center. Here $\kappa_m > 0$ when D is convex at the closest point. In addition, r_b is the bubble radius, and ν_+^ϵ and ζ are defined below in (46b) and (52), respectively. This result, which is asymptotically valid only when $r_m(t) > r_b$, shows that the bubble will collapse against ∂D on an exponentially long time scale. In §4.1, we outline the key steps in the derivation of this result using the projection method.

Once the bubble hits ∂D, it quickly becomes attached to ∂D orthogonally and its boundary becomes a circular arc in order to minimize its perimeter. Its subsequent evolution is then given by (40). However, if the length scale of the interface is sufficiently small compared to the radius of curvature of ∂D, the interface will become approximately semi-circular in shape. The motion of such a semi-circular *drop* of radius $\delta \ll 1$ has been studied in [3]. It was shown in [3] that the center of a such a small drop of radius δ, with $\delta \ll 1$ but $0 < \epsilon < \delta^3$,

satisfies the asymptotic ODE

$$\xi'(t) \sim \frac{4\epsilon^2\delta}{3\pi} K_D'(\xi(t))\,. \tag{42}$$

Here ξ is an arclength parameter for ∂D, δ is the radius of the drop, and K_D is the curvature of ∂D (positive for a convex domain D). The drop will reach a stable equilibrium, where the interface can have minimum perimeter, at a local maximum of K_D (see [2], [3], [11]).

However, the relation (40) and the drop result (42) gives no indication of the motion of a semi-circular interface intersecting a flat portion of ∂D. This case, in which metastable behavior occurs, has been studied in [36]. In §4.2 we outline the metastability analysis for a semi-circular interface located on the straight-line boundary segment joining the points $(x_L, 0)$ and $(x_R, 0)$ as shown in Fig. 4. As derived in [36], the metastable motion of the center $x_0(t)$ of the semi-circular interface satisfies the asymptotic ODE

$$\begin{aligned} x_0'(t) \;\sim\; & \frac{2\epsilon a_+^2 (\nu_+^\epsilon)^2}{\pi\beta} \left\{ \frac{K_R}{x_R - x_0} e^{-2\nu_+^\epsilon \epsilon^{-1}(x_R - x_0 - r_b)} \left(\frac{\epsilon}{2\nu_+^\epsilon}\right)^{\alpha_R+1} \Gamma(\alpha_R+1) \right. \\ & \left. - \frac{K_L}{x_0 - x_L} e^{-2\nu_+^\epsilon \epsilon^{-1}(x_0 - x_L - r_b)} \left(\frac{\epsilon}{2\nu_+^\epsilon}\right)^{\alpha_L+1} \Gamma(\alpha_L+1) \right\}. \end{aligned} \tag{43}$$

Here K_L, α_L and K_R, α_R are constants associated with the corner regions near $(x_L, 0)$ and $(x_R, 0)$, respectively. In addition, r_b is the radius of the semi-circular interface and a_+, ν_+^ϵ, and β are constants that depend on ϵ and can be calculated asymptotically for a given $Q(u)$.

4.1 Metastable Dynamics of Interior Bubbles

There are three basic steps in the projection method used in [41]. The first step is to construct a radially symmetric equilibrium bubble solution of radius r_b in all of $\mathbf{R^2}$. Then, we linearize (38) around this solution and analyze the spectrum associated with this linearization. As a result of the slight break in translation invariance, this spectrum contains exponentially small eigenvalues. Finally, we ensure that mass is conserved and that the solution to the quasi-steady linearized problem is orthogonal to the eigenspace associated with the exponentially small eigenvalues. This projection step yields an ODE for the center $\mathbf{x_0} = \mathbf{x_0}(t)$ of the bubble. We now briefly outline some of the details of this analysis.

The equilibrium bubble solution $u = U_b(r;\epsilon)$, $\sigma = \sigma_b(\epsilon)$ satisfies the radially symmetric version of (38). The solution to this problem can be constructed using

the method of matched asymptotic expansions as in [41] with the result

$$U_b(r;\epsilon) \sim \begin{cases} S_+(\epsilon) - a_+(r_b/r)^{1/2} e^{-\nu_+^\epsilon \epsilon^{-1}(r-r_b)}\,, & r > r_b\,, \\ u_0(\rho) + O(\epsilon)\,, & \rho = \epsilon^{-1}(r-r_b) = O(1)\,, \\ S_-(\epsilon) + a_-(r_b/r)^{1/2} e^{-\nu_-^\epsilon \epsilon^{-1}(r_b-r)}\,, & r < r_b\,, \end{cases} \tag{44}$$

and

$$\sigma_b(\epsilon) = \epsilon \frac{\beta}{(s_+ - s_-) r_b} + O(\epsilon^2)\,. \tag{45}$$

Here $u_0(\rho)$ satisfies (19), and $a_\pm$, β are defined in (22), (26), respectively. The constants $S_\pm$ and $\nu_\pm^\epsilon$ are given by,

$$S_\pm(\epsilon) = s_\pm - \sigma_b \nu_\pm^{-2} + O(\epsilon^2)\,, \tag{46a}$$

$$\nu_\pm^\epsilon = \nu_\pm \left[1 + \frac{\sigma_b}{2\nu_\pm^4} Q''(s_\pm) + O(\epsilon^2) \right]\,, \tag{46b}$$

where $\nu_\pm$ is defined in (21).

The quasi-steady linearization of (38) is obtained by substituting

$$u(\mathbf{x},t) = U_b\left[|\mathbf{x} - \mathbf{x_0}(t)|;\epsilon\right] + v(\mathbf{x},t)\,, \qquad \sigma(t) = \sigma_b(\epsilon) + \mu(t)\,, \tag{47}$$

into (38), where $v \ll U_b$, $v_t \ll \partial_t U_b$ and $\mu \ll \sigma_b$. Here $\mathbf{x_0}(t)$ is the unknown trajectory of the center of the bubble. This leads to the following problem for v and μ:

$$L_\epsilon v \equiv \epsilon^2 \triangle v + Q'(U_b) v = \partial_t U_b + \mu\,, \qquad \mathbf{x} \in D\,, \tag{48a}$$

$$\partial_n v = -\partial_n U_b\,, \qquad \mathbf{x} \in \partial D\,; \qquad \int_D v\, d\mathbf{x} = 0\,. \tag{48b}$$

Let (λ_j, ϕ_j) for $j \geq 0$ be the eigenpairs of the associated eigenvalue problem

$$L_\epsilon \phi = -\lambda \phi\,, \quad \mathbf{x} \in D\,; \quad \partial_n \phi = 0\,, \quad \mathbf{x} \in \partial D\,; \quad (\phi,\phi) \equiv \int_D \phi^2\, d\mathbf{x} = 1\,. \tag{49}$$

The principal eigenvalue satisfies $\lambda_0 < 0$ with $\lambda_0 = -\epsilon^2/r_b^2$ as $\epsilon \to 0$, and the corresponding eigenfunction ϕ_0 has the form $\phi_0 \sim N_0 \left(U_b' + \phi_{L0} \right)$. Here N_0 is a normalization constant and ϕ_{L0} is a boundary layer function, localized near ∂D, which allows $\partial_n \phi_0 = 0$ on ∂D to be satisfied. In addition, as a result of the near translation invariance and the exponential decay behavior (44), there are two exponentially small eigenvalues λ_1 and λ_2. The corresponding eigenfunctions are given asymptotically by $\phi_j \sim N_j \left(\partial_{x_j} U_b + \phi_{Lj} \right)$ for some boundary layer functions ϕ_{Lj}, $j = 1, 2$. Here we have set $x_1 = x$ and $x_2 = y$. A boundary layer analysis determines ϕ_{Lj} for $j = 0, 1, 2$ and hence we can obtain explicit asymptotic formulas for ϕ_j on ∂D for $j = 0, 1, 2$ (see [41]).

Next, we expand the solution $v(\mathbf{x},t)$ to (48) in terms of the eigenfunctions ϕ_j of (49) as $v(\mathbf{x},t) = \sum_{j=0}^{\infty} c_j\phi_j/\lambda_j$. The coefficients $c_j = c_j(t)$ for $j \geq 0$ are given by

$$c_j = -(\partial_t U_b, \phi_j) - \mu\,(1,\phi_j) - \epsilon^2 \int_{\partial D} \phi_j \partial_n U_b \, ds\,, \tag{50}$$

where $(f,g) \equiv \int_D fg\, d\mathbf{x}$. Since U_b and ϕ_j, for $j = 0,..,N$, are known when $\epsilon \ll 1$, we can calculate the inner products and the boundary integral in (50) asymptotically to determine c_j for $j = 0,1,2$.

The conditions to determine $\mu(t)$ and $\mathbf{x_0}(t)$ are as follows. First, we must ensure that $\int_D v\, d\mathbf{x} = 0$ in order to conserve mass. Since ϕ_0 is of one sign, this condition requires that v has no component in the direction of ϕ_0. Hence, $c_0(t) \equiv 0$, which then determines μ. Thus, the existence of the negative eigenvalue λ_0 for (49) does not lead to an instability of the bubble solution. We remark that if mass was not conserved, the bubble would shrink to a point under a mean curvature flow on a time scale $|\lambda_0^{-1}| = O(\epsilon^{-2})$ (see [14]). Next, since λ_j for $j = 1,2$ are exponentially small as $\epsilon \to 0$, we must also require that the limiting solvability conditions $c_j \to 0$ as $\epsilon \to 0$ for $j = 1,2$ be satisfied. These conditions yield a differential equation for $\mathbf{x_0}(t)$ that governs the metastable bubble motion.

In this way, it was obtained in [41] that for a bubble strictly contained in D, the center $\mathbf{x_0}(t)$ of the bubble satisfies the asymptotic ODE

$$\mathbf{x_0}' \sim \frac{\epsilon a_+^2 \nu_+^2}{\pi\beta} \int_{\partial D} r^{-1} e^{-2\nu_+^{\epsilon}(r-r_b)/\epsilon}\, \hat{\mathbf{r}}\, [1 + \hat{\mathbf{r}}\cdot\hat{\mathbf{n}}]\, \hat{\mathbf{r}}\cdot\hat{\mathbf{n}}\, ds\,. \tag{51}$$

Here $r = |\mathbf{x}(\xi) - \mathbf{x_0}(t)|$, $\hat{\mathbf{r}} = (\mathbf{x}(\xi) - \mathbf{x_0}(t))/r$, and $\hat{\mathbf{n}} = \hat{\mathbf{n}}(\xi)$ is the unit outward normal to ∂D, where ξ parameterizes ∂D. Also, β and ν_+^{ϵ} are defined in (26) and (46b).

The (unstable) equilibrium location $\mathbf{x_{0e}}$ for the bubble center is obtained by setting $\mathbf{x_0}' = 0$ in (51). For a strictly convex domain, this yields that $\mathbf{x_{0e}}$ is located at an $O(\epsilon)$ distance from the center of the largest inscribed circle for D (see [41]). Finally, by using Laplace's method on (51) it is clear that the metastable bubble dynamics is determined largely in terms of local information from the point $\mathbf{x}(\xi_0)$ on ∂D nearest to $\mathbf{x}_0$. In this way, it is shown in [41] that the bubble drifts towards the closest point on ∂D and the distance $r_m(t) = |\mathbf{x}(\xi_0) - \mathbf{x_0}(t)|$ between the bubble center and the closest point satisfies (41), where ζ in (41) is given by

$$\zeta = \frac{2a_+^2\nu_+^2}{\pi\beta}\left(\frac{\pi}{\nu_+^{\epsilon}}\right)^{1/2}\,. \tag{52}$$

4.2 Metastable Dynamics of Attached Bubbles

We now characterize the metastable dynamics of a semi-circular interface of radius r_b that intersects a flat portion of ∂D as shown in Fig. 4. The flat portion of ∂D is taken to be the straight-line segment between $(x_L, 0)$ and $(x_R, 0)$.

The interface is centered around $\mathbf{x}_0 = (x_0, 0)$ where $x_L < x_0 < x_R$. We let $\partial D = \partial D_c \cup \partial D_s$ where ∂D_s refers to the straight-line segment of the boundary and ∂D_c denotes the remaining curved part of ∂D. The distance between the interface and ∂D_c is assumed to be a minima at either of the two corners $(x_L, 0)$ or $(x_R, 0)$.

Near the corner points, ∂D is assumed to have the following local behavior

$$\text{near } (x_L, 0)\,;\; y = \psi_L(x), \qquad \psi_L'(x) \sim -K_L(x_L - x)^{\alpha_L}, \;\; \text{as } x \to x_L^-, \tag{53a}$$

$$\text{near } (x_R, 0)\,;\; y = \psi_R(x), \qquad \psi_R'(x) \sim K_R(x - x_R)^{\alpha_R}, \;\; \text{as } x \to x_R^+, \tag{53b}$$

$$\tag{53c}$$

where $\alpha_L > 0$ and $\alpha_R > 0$. When $\alpha_L = \alpha_R = 1$, K_L and K_R are proportional to the curvatures of ∂D_c at the corners.

In [36] the projection method was used to determine the motion of the semi-circular interface. The outline of the analysis is as follows. First, we construct a radially symmetric equilibrium solution to (38) as in (44). This equilibrium solution is centered at $(x_0, 0)$ and it corresponds to the semi-circular interface. We then linearize the equation around U_b as in (47), where $\mathbf{x_0}(t) = (x_0(t), 0)$. This yields the linearized problem (48). The associated eigenvalue problem has a principal eigenvalue $\lambda_0 = -\epsilon^2/r_b^2$. In addition, due to the near translation invariance in the horizontal direction x, there is one exponentially small eigenvalue corresponding to the approximate eigenfunction $\phi_1 \sim \partial_x U_b$. The conservation of mass condition determines the correction μ to the Lagrange multiplier parameter σ. In addition, a limiting solvability condition, which requires that v be orthogonal to the eigenfunction associated with the exponentially small eigenvalue must be imposed. This yields the following asymptotic differential equation for $x_0(t)$:

$$x_0'(t) \sim \frac{2\epsilon a_+^2 (\nu_+^\epsilon)^2}{\pi\beta} \int_{\partial D} \frac{(x - x_0)}{r^2} e^{-2\nu_+^\epsilon \epsilon^{-1}(r - r_b)} \hat{\mathbf{r}} \cdot \hat{\mathbf{n}}\, ds\,. \tag{54}$$

Here $\hat{\mathbf{r}} = (\mathbf{x} - \mathbf{x_0})/r$, $\mathbf{x_0} = (x_0, 0)$, $r = |\mathbf{x} - \mathbf{x_0}|$ and $\hat{\mathbf{n}}$ is the unit outward normal to ∂D. Also, β and ν_+^ϵ are given in (26) and (46b), respectively. Since, $\hat{\mathbf{r}}$ and $\hat{\mathbf{n}}$ are orthogonal on the straight-line segment ∂D_s of ∂D, the integral in (54) is an integral over the curved segment ∂D_c. For $\epsilon \to 0$, the dominant contribution to this integral arises from the corner regions $(x_L, 0)$ and $(x_R, 0)$. Laplace's method and the local information (53) can then be used to obtain the explicit differential equation (43) for $x_0(t)$.

Thus, the ODE (43) for $x_0(t)$ shows that the motion of the center of the semi-circular interface along the straight-line boundary segment between $(x_L, 0)$ and $(x_R, 0)$ is determined by the shape of the boundary at these corner points and by the distance from the interface to these points. The interface will move, without change of shape, until a stable steady state is reached or until the interface touches $(x_L, 0)$ or $(x_R, 0)$. If the interface reaches the curved part of the boundary, it will subsequently continue to evolve according to (40).

4.3 An Explicit Example of an Attached Bubble

When $K_L K_R > 0$, we obtain from (43) that there is a unique steady-state solution x_{0e}, satisfying $x_L < x_{0e} < x_R$. For $\epsilon \to 0$, a two-term approximation for x_{0e} is

$$x_{0e} \sim \frac{x_L + x_R}{2} + \frac{\epsilon}{4\nu_+^\epsilon} \log \left[\frac{K_L \Gamma(\alpha_L + 1)}{K_R \Gamma(\alpha_R + 1)} \left(\frac{\epsilon}{2\nu_+^\epsilon} \right)^{\alpha_L - \alpha_R} \right] + O(\epsilon^2) \,. \tag{55}$$

This steady state is stable when $K_L < 0$, $K_R < 0$, and is unstable when $K_L > 0$, $K_R > 0$. Specifically, this shows that if D is convex near $(x_L, 0)$ and $(x_R, 0)$, then there is no stable equilibrium location on ∂D_s. There is no equilibrium solution if $K_L K_R < 0$.

To illustrate the slow dynamics, let $Q(u) = 2(u - u^3)$. Then, we calculate that

$$\nu_\pm^\epsilon = 2[1 - \epsilon(4r_b)^{-1} + \cdots] \,, \quad a_\pm = 2 \,, \quad s_\pm = \pm 1 \,, \quad \beta = 4/3 \,. \tag{56}$$

Suppose that $\alpha_L = \alpha_R = \alpha$. Then, from (43) the center $x_0(t)$ of the semi-circular interface satisfies

$$x_0' \sim c \left[\frac{K_R}{x_R - x_0} e^{-2\nu_+^\epsilon \epsilon^{-1}(x_R - x_0 - r_b)} - \frac{K_L}{x_0 - x_L} e^{-2\nu_+^\epsilon \epsilon^{-1}(x_0 - x_L - r_b)} \right] , \tag{57}$$

where

$$c = \frac{6\epsilon^{\alpha+2}\Gamma(\alpha+1)}{4^\alpha \pi} \,. \tag{58}$$

The steady state location for x_0, when $K_L K_R > 0$, is

$$x_{0e} \sim \frac{x_L + x_R}{2} + \frac{\epsilon}{8} \log \left(\frac{K_L}{K_R} \right) . \tag{59}$$

For the initial value, $x(0) = x_0^0$, the qualitative properties of the dynamics associated with (57) are as follows. When $K_L > 0$ and $K_R > 0$, $x_0(t)$ moves exponentially slowly towards x_L if $x_0^0 < x_{0e}$, or towards x_R if $x_0^0 > x_{0e}$ (see Fig. 5). When $K_L < 0$ and $K_R < 0$, $x_0(t)$ will approach the stable steady state at x_{0e} for any initial condition (see Fig. 6). If $K_L < 0$ and $K_R > 0$, then $x_0(t)$ will move towards x_R as shown in Fig. 7. Finally, $x_0(t)$ will move towards x_L if $K_L > 0$ and $K_R < 0$. In each case, the interface moves in the direction that will allow its perimeter to decrease. When the interface reaches the corner points $(x_L, 0)$ or $(x_R, 0)$, the subsequent evolution of the interface is determined by (40).

5 Slow Spike Motion for the Shadow Problem

Turing [39] proposed a reaction-diffusion system of activator-inhibitor type to mathematically model morphogenesis. From a linear stability analysis he suggested that such a system could have stable inhomogeneous solutions with isolated peaks in the inducer concentration. Subsequent studies (e.g. [15], [17]),

which have involved large-scale numerical computations, have shown that robust spike-type patterns in the activator concentration are possible when the activator diffuses much more slowly than the inhibitor.

In [18], spike-type solutions are analyzed for an activator-inhibitor system known as the Gierer-Meinhardt model [15]. In scaled and dimensionless variables, this model is formulated as

$$a_t = \epsilon^2 \triangle a - a + \frac{a^p}{h^q}\,, \qquad \mathbf{x} \in D \subset \mathbf{R^N}\,, \tag{60a}$$

$$\tau h_t = k_h \triangle h - \mu h + \epsilon^{-N} a^m\,, \qquad \mathbf{x} \in D \subset \mathbf{R^N}\,, \tag{60b}$$

$$a_n = 0\,, \qquad h_n = 0\,, \qquad \mathbf{x} \in \partial D\,. \tag{60c}$$

Here $\epsilon \ll 1$, a and h are the activator and inhibitor concentrations, respectively, D is a bounded domain in $\mathbf{R^N}$, and the derivatives in $(60c)$ are the normal derivatives to the boundary of D. Also, $\tau > 0$, $\mu > 0$ and the exponents satisfy

$$1 < p < 1 + mq, \qquad q > 0, \qquad m > 0\,.$$

There are only a few partial results for (60) in the fully nonlinear regime. A survey of some of these results are given in [29].

In [18], the weak coupling limit $k_h \gg 1$ for (60) is analyzed. This limit, together with the assumption that the dynamics of a are much slower than those of h, i.e. $\tau \ll 1$, leads to the following non-local problem for a, known as the shadow problem ([28], [29]):

$$a_t = \epsilon^2 \triangle a - a + \frac{a^p}{h^q} \qquad \mathbf{x} \in D \subset \mathbf{R^N}\,, \tag{61a}$$

$$h = \frac{\epsilon^{-N}}{\mu |D|} \int_D a^m \, d\mathbf{x}\,, \tag{61b}$$

$$a_n = 0\,, \qquad \mathbf{x} \in \partial D\,. \tag{61c}$$

Here $|D|$ is the volume of D.

For the equilibrium problem, we let $a = h^\gamma u$ in (61a), where $\gamma = q/(p-1)$, to obtain the following problem for u:

$$\epsilon^2 \triangle u - u + u^p = 0\,, \qquad x \in D\,; \qquad u_n = 0\,, \qquad \mathbf{x} \in \partial D\,. \tag{62}$$

Assume that $p < p_c(N)$, where $p_c(N)$ is the critical Sobolev exponent. Then (62) admits a solution with M spikes, where the spikes are located near some points $\mathbf{x_{0i}}$ for $i = 1, .., M$ in D that are to be determined. For a solution with a spike on the boundary of the domain, it was proved in [28] that the spike can be located at the point on ∂D where the mean curvature of ∂D is the largest. In [42], the projection method was used to construct a one-spike solution to (62) where the spike is contained strictly within D. It was shown that, for a convex domain, the spike is located at an $O(\epsilon)$ distance from the center of

the largest inscribed sphere for D. This analysis required exponential precision since the spike-layer solution decays exponentially away from its core and hence interacts with the boundary only by exponentially small terms. More recently, the important papers of [7], [16] and [20] have proved that the problem for the determination of the locations of the spikes for a multi-spike solution is intimately connected with the geometric problem of the lattice packing of balls of equal radii inside D.

In [18] the projection method is used to show that (61) can support a metastable spike-layer solution. If the spike is initially localized near some point $\mathbf{x_0}(0)$ in D, then this spike will move exponentially slowly towards the closest point on the boundary ∂D. This result is critically dependent on the non-local nature of (61), which precludes the existence of an unstable mode with an $O(1)$ eigenvalue for the corresponding linearized problem. We now briefly outline the analysis in [18].

A one-spike equilibrium solution to (61) in $\mathbf{R^N}$ is represented by

$$a = a_E(\mathbf{x};\mathbf{x_0}) \equiv h^\gamma u_c(|\mathbf{x}-\mathbf{x_0}|) \qquad \gamma = q/(p-1)\,. \tag{63}$$

Here the radially symmetric function $u_c(\rho)$, called the canonical spike solution, satisfies the radially symmetric version of (62)

$$u_c'' + \frac{(N-1)}{\rho}u_c' - u_c + u_c^p = 0\,, \tag{64a}$$

$$u_c'(0) = 0 \quad \text{and} \quad u_c(\infty) = 0\,, \tag{64b}$$

$$u_c(\rho) \sim a\rho^{(1-N)/2}e^{-\rho}\,, \quad \text{as} \quad \rho \to \infty\,. \tag{64c}$$

In terms of this solution, h is given by

$$h = \left(\frac{\Omega_N}{\mu|D|}\int_0^\infty u_c^m \rho^{N-1}d\rho\right)^{\frac{p-1}{(p-1)-qm}}\,, \tag{65}$$

where Ω_N is the surface area of the unit N dimensional sphere. Since a_E satisfies the steady-state problem for (61a), but fails to satisfy the no flux boundary condition (61c) by only exponentially small terms for any value of $\mathbf{x_0} \in D$, we expect that the spectrum of the eigenvalue problem associated with the linearization about a_E contains exponentially small eigenvalues. The non-local nature of (61) will ensure that these exponentially small eigenvalues are the principal eigenvalues of the linearization.

The non-local eigenvalue problem for the linearization is obtained by introducing ϕ and η defined by

$$a(\mathbf{x},t) = a_E(\mathbf{x};\mathbf{x_0}) + e^{-\lambda t}\phi(\mathbf{x}), \tag{66a}$$

$$h(\mathbf{x},t) = h + e^{-\lambda t}\eta(\mathbf{x})\,. \tag{66b}$$

Here $\phi \ll a_E$ and $\eta \ll h$. From (61) this yields the non-local eigenvalue problem in D:

$$L_\epsilon \phi \equiv \epsilon^2 \triangle \phi + (-1 + p u_c^{p-1})\phi - \frac{mq\epsilon^{-N} u_c^p}{\beta_N \Omega_N} \int_D u_c^{m-1} \phi \, d\mathbf{x} = -\lambda \phi, \quad (67a)$$

$$\phi_n = 0 \quad \text{on} \quad \partial D \,. \quad (67b)$$

Here, β_N is defined by

$$\beta_N = \int_0^\infty u_c^{m-1} \rho^{N-1} \, d\rho \,. \quad (68)$$

Since u_c is localized near $\mathbf{x} = \mathbf{x_0}$, we only seek eigenfunctions of (67) that are localized near $x = x_0$. These eigenfunctions have the form

$$\tilde{\phi}(\mathbf{y}) = \phi(\mathbf{x_0} + \epsilon \mathbf{y}) \,, \qquad \mathbf{y} = \epsilon^{-\mathbf{1}}(\mathbf{x} - \mathbf{x_0}) \,. \quad (69)$$

They satisfy the corresponding infinite domain problem in $\mathbf{R^N}$,

$$\tilde{L}_\epsilon \tilde{\phi} \equiv \triangle_y \tilde{\phi} + (-1 + p u_c^{p-1})\tilde{\phi} - \frac{mq u_c^p}{\beta_N \Omega_N} \int_{\mathbf{R^N}} u_c^{m-1} \tilde{\phi} \, d\mathbf{y} = -\tilde{\lambda} \tilde{\phi}, \quad (70a)$$

$$\tilde{\phi} \to 0 \qquad \text{as} \quad |\mathbf{y}| \to \infty \,, \quad (70b)$$

where $u_c = u_c(|\mathbf{y}|)$.

We now outline the key properties of the spectrum associated with (67) and (70). Define $\tilde{\phi}_i \equiv \partial_{y_i} u_c(|\mathbf{y}|)$. Then, from translation invariance and symmetry considerations, which shows that the integral in (70) vanishes when $\tilde{\phi} = \tilde{\phi}_i$, it follows that $\tilde{\phi}_i$ for $i = 1, .., N$ satisfies (70) with $\tilde{\lambda} = 0$. Here y_i is the i^{th} coordinate of $\mathbf{y}$. Thus, (70) has a zero eigenvalue of multiplicity N with corresponding eigenfunctions $\tilde{\phi}_i = \partial_{y_i} u_c(|\mathbf{y}|)$ for $i = 1, .., N$. Since $\mathbf{x_0} \in D$, and u_c is exponentially localized, these eigenpairs will be perturbed by only exponentially small terms as a result of the finite domain in the eigenvalue problem (67). More precisely, it was shown in [18] that (67) has N exponentially small eigenvalues with corresponding eigenfunctions given by $\phi_i \sim \partial_{x_i} u_c + \phi_{Li}$, where ϕ_{Li} is a boundary layer function localized near ∂D that allows the boundary condition in (67b) to be satisfied. An analysis using Green's identity shows that these exponentially small eigenvalues for (67) are given for $\epsilon \to 0$ by

$$\lambda_i \sim -\frac{\epsilon a^2 N}{\hat{\beta}_N \Omega_N} \int_{\partial D} (x_i - x_{0i})^2 r^{-(1+N)} e^{-2r/\epsilon} (\hat{\mathbf{r}} \cdot \hat{\mathbf{n}})(1 + \hat{\mathbf{r}} \cdot \hat{\mathbf{n}}) \, dS \,, \quad (71)$$

for $i = 1, .., N$. Here $r = |\mathbf{x} - \mathbf{x_0}|$, $\hat{\mathbf{r}} = (\mathbf{x} - \mathbf{x_0})/r$, x_i is the i^{th} coordinate of $\mathbf{x}$, and $\hat{\mathbf{n}}$ is the unit outward normal to ∂D. Also, a is given in (64c) and $\hat{\beta}_N$ is defined by

$$\hat{\beta}_N = \int_0^\infty \left[u_c'(\rho) \right]^2 \rho^{N-1} \, d\rho \,. \quad (72)$$

An asymptotic evaluation of (71) using Laplace's method then shows that λ_i is determined by local information from the point on ∂D that is closest to the center $\mathbf{x_0}$ of the spike.

The other key property of the spectrum concerns the principal eigenpair for (67). When the non-local term in (70) is absent, it is well-known that the local problem has an $O(1)$ negative eigenvalue $\tilde{\lambda}_0$ with a corresponding radially symmetric eigenfunction $\tilde{\phi}_0(\rho)$. In [18] we used a path-following method to numerically compute this eigenvalue in terms of a homotopy parameter δ, where δ with $0 \le \delta \le 1$, multiplies the non-local integral term in (70). In this way the effect of the non-local term is gradually introduced. It was shown in [18] that the eigenvalue branch as a function of δ, which emanates from $\tilde{\lambda}_0$, has crossed into the right-half plane when $\delta = 1$. Hence, the effect of the non-local term is to ensure that the principal eigenvalue of (70) is the zero eigenvalue of translation. In this way, it was shown that the principal eigenvalue of (67) is exponentially small as $\epsilon \to 0$.

The final step in the analysis of metastable spike motion is to linearize (61) around the quasi-equilibrium solution by writing

$$a(\mathbf{x},t) = a_E(\mathbf{x};\mathbf{x_0}(t)) + w(\mathbf{x},t)\,, \tag{73}$$

where a_E is defined in (63), and $w \ll a_E$ and $w_t \ll \partial_t a_E$. The linearized problem is

$$L_\epsilon w = \partial_t a_E \quad \text{in} \quad D\,, \tag{74a}$$

$$\partial_n w = -\partial_n a_E\,, \quad \text{on} \quad \partial D\,, \tag{74b}$$

where L_ϵ is defined in (67a). By applying a limiting solvability condition that requires that w is orthogonal to the eigenfunctions associated with the exponentially small eigenvalues, the following ODE for the trajectory $\mathbf{x_0} = \mathbf{x_0}(t)$ was derived in [18]:

$$\mathbf{x_0}' \sim \frac{\epsilon N a^2}{\hat{\beta}_N \Omega_N} \int_{\partial D} \hat{\mathbf{r}}\, r^{1-N} e^{-2r/\epsilon} (1 + \hat{\mathbf{r}}\cdot\hat{\mathbf{n}})\, \hat{\mathbf{r}}\cdot\hat{\mathbf{n}}\, dS\,. \tag{75}$$

Finally, assume that there is a unique point on ∂D, labelled by $\mathbf{x_m}$ such that the distance from $\mathbf{x_0}$ to ∂D is mimimized. Then, upon using Laplace's method on (75), it was shown in [18] that the spike-layer moves monotonically, but exponentially slowly, in a straight line towards the point $\mathbf{x_m}$ on ∂D and that the distance $r_m(t) \equiv |\mathbf{x_m} - \mathbf{x_0}(t)|$ satisfies the asymptotic ODE

$$r_m' \sim -\zeta r_m \left(\frac{\epsilon}{r_m}\right)^{(N+1)/2} H(r_m)\, e^{-2r_m/\epsilon}\,. \tag{76}$$

Here ζ is defined by

$$\zeta = \frac{2Na^2}{\Omega_N \hat{\beta}_N} \pi^{(N-1)/2}\,. \tag{77}$$

The function $H(r_m)$ is given in terms of the principal radii of curvature R_i, $i = 1, .., N-1$, of the boundary ∂D at the closest point $\mathbf{x_m} \in D$ by,

$$H(r_m) \equiv (1 - r_m/R_1)^{-1/2} (1 - r_m/R_2)^{-1/2} \dots (1 - r_m/R_{N-1})^{-1/2} . \qquad (78)$$

The main result (76), which is very similar to the result in §4 for the motion of bubble solutions for the constrained Allen-Cahn equation, shows that the spike will take an asymptotically exponentially long time to reach ∂D when $\epsilon \ll 1$.

6 A Combustion Problem

There are several other non-local models arising in different branches of science where localized structures evolve on exponentially long time scales. Two such problems are the evolution of hot spots in microwave heated ceramic materials (see [21] for the model) and the evolution of flame-fronts in a vertical channel.

In particular, in [30] an evolution equation describing the upward propagation of a flame-front in a vertical channel, subject to buoyancy effects, was derived. Suppose that the vertical channel has a constant cross-section D in the (x_1, x_2) plane and let the positive z axis be perpendicular to this cross-section and in the direction of propagation of the flame. Then, in terms of dimensionless variables, and in a particular asymptotic regime, the flame-front interface $z = \Phi(x_1, x_2, t)$ was found in [30] to satisfy the non-local problem

$$\Phi_t - \frac{1}{2}|\nabla\Phi|^2 = \epsilon\triangle\Phi + \Phi - \frac{1}{|D|}\int_D \Phi \, d\mathbf{x} , \qquad \mathbf{x} \in D \in \mathbf{R^2} , \qquad (79a)$$

$$\partial_n\Phi = 0 , \qquad \mathbf{x} \in \partial D . \qquad (79b)$$

Here $\epsilon \ll 1$, $\mathbf{x} = (x_1, x_2)$, $|D|$ is the area of the cross-section and ∂_n is the outward normal derivative. Some experimental pictures of the flame-fronts are shown in [23]. These pictures show that the flame-front assumes a roughly paraboloidal shape and that the tip of the front moves slowly.

The simpler one-dimensional problem in a slab geometry was studied in [9] and [37]. In this case, $\Phi = \Phi(x, t)$ and (79) reduces on the strip $0 < x < 1$, $t > 0$ to

$$\Phi_t - \frac{1}{2}\Phi_x^2 = \epsilon\Phi_{xx} + \Phi - \int_0^1 \Phi \, dx , \qquad \Phi_x(0, t) = \Phi_x(1, t) = 0 . \qquad (80)$$

Certain special classes of solutions of (80), corresponding to concave interface shapes were shown in [9] and [37] to be metastable. In particular, in [37] it was shown that the tip $x_0 = x_0(t)$ of a parabolic flame-front interface drifts exponentially slowly towards the closest point on the channel wall (i.e. either $x = 0$ or $x = 1$) according to the differential equation

$$x_0' \sim \sqrt{\frac{2}{\pi\epsilon}} \left[\left((1 - x_0)^2 + \frac{\pi^2\epsilon}{3} \right) e^{-(1-x_0)^2/2\epsilon} - (x_0^2 + \frac{\pi^2\epsilon}{3}) e^{-x_0^2/2\epsilon} \right] . \qquad (81)$$

The analysis in [37] leading to (81) was based on converting the non-local problem (80) to a local problem by applying the transformation $v = -\Phi_x$, which yields the Burgers-Sivashinsky equation

$$v_t + vv_x - v = \epsilon v_{xx}\,, \qquad v(0,t) = v(1,t) = 0\,. \tag{82}$$

The problem (79), and its one-dimensional counterpart (80), seem quite different in form from the quasi-linear problems considered in §3-5. However, this is really not the case. In fact, the transformation

$$\Phi = 2\epsilon \ln u \tag{83}$$

reduces (79) to the non-local problem

$$u_t = \epsilon \triangle u + u\left(\ln u - \frac{1}{|D|}\int_D \ln u\, d\mathbf{x}\right)\,, \qquad \mathbf{x} \in D\,, \tag{84a}$$

$$\partial_n u = 0\,, \qquad \mathbf{x} \in \partial D\,. \tag{84b}$$

This problem is similar to those considered earlier, but has yet to be analyzed.

Acknowledgements

It is my pleasure to acknowledge the contributions of my graduate students David Iron, Doug Stafford and Xiaodi Sun to some of the work described in this article. The support of NSERC grant 5-81541 is also gratefully acknowledged.

References

[1] N. Alikakos, P.W. Bates, G. Fusco, *Slow Motion for the Cahn-Hilliard Equation in One Space Dimension*, J. Diff. Equat. 90, (1991), pp. 81-135.

[2] N. Alikakos, L. Bronsard, G. Fusco, *Slow motion in the Gradient Theory of Phase Transitions via Energy and Spectrum*, Calc. Var. Partial Differential Equations Vol. 6, No. 1, (1998), pp. 39-66.

[3] N. Alikakos, X. Chen, G. Fusco, *Motion of a Drop by Surface Tension Along the Boundary*, preprint.

[4] N. Alikakos, G. Fusco, *Some Aspects of the Dynamics of the Cahn-Hilliard Equation*, Resenhas Vol. 1, No. 4, (1994), pp. 517-530.

[5] N. Alikakos, G. Fusco, *Slow Dynamics for the Cahn-Hilliard Equation in Higher Spatial Dimensions, Part 2: the Motion of Bubbles*, to appear, Arch. Rational Mech. Anal. (1998).

[6] N. Alikakos, G. Fusco, M. Kowalczyk, *Finite Dimensional Dynamics and Interfaces Intersecting the Boundary: Equilibria and Quasi-Invariant Manifold*, Indiana Univ. Math. J. 45, No. 4, (1996), pp. 1119-1155.

[7] P. W. Bates, G. Fusco, *Equilibria with Many Nuclei for the Cahn-Hilliard Equation*, preprint (1998).

[8] P. W. Bates, J. Xun, *Metastable Patterns for the Cahn-Hilliard Equation: Parts 1 and 2*, J. Diff. Equat. 111, (1994), pp. 421-457; J. Diff. Equat. 117, (1995), pp. 165–216.

[9] H. Berestycki, S. Kamin, G. Sivashinsky, *Nonlinear Dynamics and Metastability in a Burgers Type Equation*, Compte Rendus Acad. Sci., Paris t. 321, Serié 1, (1995), pp. 185-190.

[10] J. Carr, R. Pego, *Metastable Patterns in Solutions of* $u_t = \epsilon^2 u_{xx} - f(u)$, Comm. Pure Appl. Math. 42, (1989), pp. 523-576.

[11] X. Chen, M. M. Kowalczyk, *Existence of Equilibria for the Cahn-Hilliard Equation via Local Minimizers of the Perimeter*, Comm. Partial Differential Equat. 21, No. 7-8, (1996), pp. 1207-1233.

[12] G. Fusco, J. K. Hale, *Slow Motion Manifolds, Dormant Instability and Singular Perturbations*, J. Dyn. Diff. Equat. 1, (1989), pp. 75-94.

[13] M. Gage, *On an Area-Preserving Evolution For Plane Curves*, Contemp. Math. 51, (1986), pp. 51-62.

[14] M. Gage, R.S. Hamilton, *The Heat Equation Shrinking Convex Plane Curves*, J. Diff. Geom. 23, (1986), pp. 69-96.

[15] A. Gierer, H. Meinhardt, *A Theory of Biological Pattern Formation*, Kybernetik, Vol. 12, (1972), pp. 30-39.

[16] C. Gui, J. Wei, *Multiple Interior Peak Solutions for some Singularly Perturbed Neumann Problems*, preprint (1998).

[17] D. Holloway, *Reaction-diffusion Theory of Localized Structures with Application to Vertebrate Organogenesis*, Ph. D Thesis (Chemistry), University of British Columbia, Vancouver, (1995).

[18] D. Iron, M. J. Ward, *A Metastable Spike Solution for a Non-Local Reaction-Diffusion Model*, submitted SIAM J. Appl. Math. (1998).

[19] M. Kowalczyk, *Exponentially Slow Dynamics and Interfaces Intersecting the Boundary*, J. Diff. Eq. 138, No. 1, (1997), pp. 55-85.

[20] M. Kowalczyk, *Multiple Spike Layers in the Shadow Gierer-Meinhardt System: Existence of Equilibria and Approximate Invariant Manifold*, preprint (1998).

[21] G. Kriegsmann, *Hot Spot Formation in Microwave Heated Ceramic Fibers*, IMA J. Appl. Math. 59, (1997), pp. 123-148.

[22] J. Laforgue, R.E. O'Malley, *On the Motion of Viscous Shocks and the Super-Sensitivity of Their Steady-State Limits*, Methods and Appl. of Anal. 1, (1994), pp. 465-487.

[23] E. von Lavante, R.A. Strehlow, *The Mechanism of Lean Limit Flame Extinction* , Combustion and Flame, 49, (1983), pp. 123-140.

[24] D. Ludwig, *Persistence of Dynamical Systems under Random Perturbations*, SIAM Review 17, (1975), pp. 605-640.

[25] R.S. Maier, D.L. Stein, *Limiting Exit Location Distributions in the Stochastic Exit Problem*, SIAM J. Appl. Math. 57 No. 3, (1997), pp. 752-790.

[26] H. Matano, *Asymptotic Behavior and Stability of Semilinear Diffusion Equations*, Publ. Res. Inst. Math., Kyoto, 15, (1979), pp. 401-451.

[27] B.J. Matkowsky, Z. Schuss, *The Exit Problem for Randomly Perturbed Dynamical Systems*, SIAM J. Appl. Math. 33, (1977), pp. 365-382.

[28] W. M. Ni, *On the Shape of Least-Energy Solutions to a Semilinear Neumann Problem*, Comm. Pure Appl. Math, Vol. XLIV, (1991), pp. 819-851.

[29] W. M. Ni, *Diffusion, Cross-Diffusion, and their Spike-Layer Steady-States*, Notices of the AMS, Vol. 45, No. 1, (1998), pp. 9-18.

[30] Z. Rakib, G.I. Sivashinsky, *Instabilities in Upward Propagating Flames*, Combust. Sci. and Tech. 54, (1987), pp. 69-84.

[31] L. G. Reyna, M. J. Ward, *On the Exponentially Slow Motion of a Viscous Shock*, Comm. Pure Appl. Math. 48, (1995), pp. 79-120.

[32] L. G. Reyna, M.J. Ward, *Metastable Internal Layer Dynamics for the Viscous Cahn-Hilliard Equation*, Methods and Appl. of Anal. 2, No. 3, (1995), pp. 285-306.

[33] J. Rubinstein, P. Sternberg, *Nonlocal Reaction-Diffusion Equations and Nucleation*, IMA J. Appl. Math. Vol. 48, (1992), pp. 249-264.

[34] J. Rubinstein, P. Sternberg, J. Keller, *Fast Reaction, Slow Diffusion, and Curve Shortening*, SIAM J. Appl. Math. Vol. 49, No. 1, (1989), pp. 116-133.

[35] D. Stafford, M. J. Ward, *Metastable Dynamics for the Allen-Cahn Equation in Dumbbell-Shaped Domains*, submitted, Studies in Appl. Math. (1998).

[36] D. Stafford, M. J. Ward, B. Wetton, *Motion of Attached Bubbles for the Constrained Allen-Cahn Equation*, submitted, Europ. J. Appl. Math. (1998).

[37] X. Sun, M. J. Ward, *Metastability for a Generalized Burgers Equation with Applications to Propagating Flame-Fronts*, to appear, Europ. J. Appl. Math. (1998).

[38] X. Sun, M. J. Ward, *Exponentially Ill-Conditioned Convection-Diffusion Equations in Multi-Dimensional Domains*, submitted, Methods and Appl. of Analy. (1998).

[39] A. Turing, *The Chemical Basis of Morphogenesis*, Phil. Trans. Roy. Soc. B, 327, (1952), pp. 37-72.

[40] M. J. Ward, *Metastable Patterns, Layer Collapses, and Coarsening for a One-Dimensional Ginzburg-Landau Equation*, Stud. Appl. Math. 91, (1994), pp. 51-93.

[41] M. J. Ward, *Metastable Bubble Solutions for the Allen-Cahn Equation with Mass Conservation*, SIAM J. Appl. Math. Vol. 56, No. 5, (1996), pp. 1247–1279.

[42] M. J. Ward, *An Asymptotic Analysis of Localized Solutions for some Reaction-Diffusion Models in Multi-Dimensional Domains*, Stud. Appl. Math Vol. 97 No. 2, (1996), pp. 103-126.

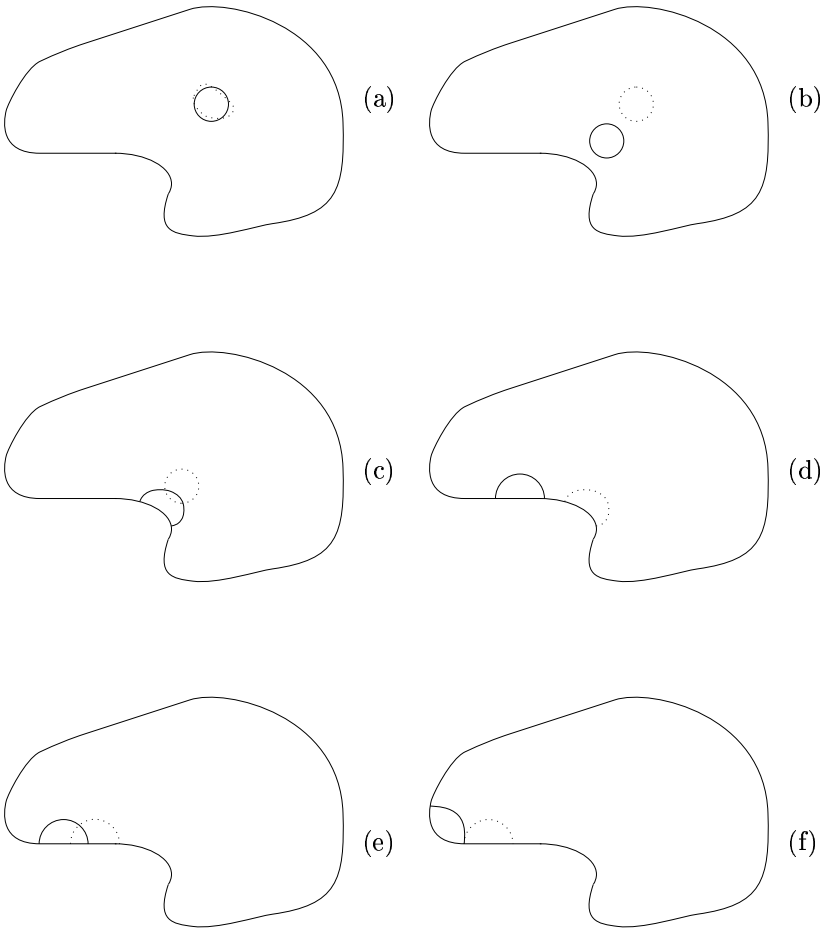

Figure 3: Evolution of a small convex interface inside a domain D. (a) The convex interface evolves by (40) into a circle. (b) The circular interface drifts, satisfying (41), towards the closest point on ∂D. (c) The interface attaches to ∂D, intersecting orthogonally. (d) The interface moves along ∂D satisfying (40). (e) If the interface encounters a flat portion of ∂D, it moves along this flat portion according to (43). (f) When a curved part of ∂D is reached, the interface again evolves by (40) until a steady state is attained, which is centered near a local maximum of the curvature of ∂D.

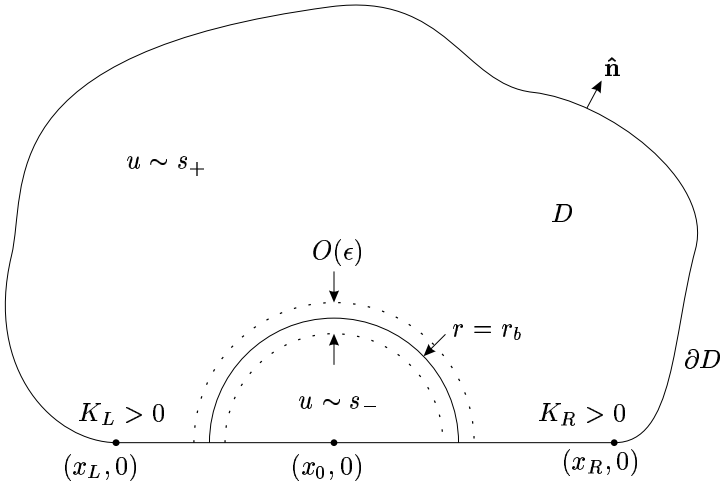

Figure 4: Plot of a two-dimensional domain D with a flat boundary segment and a semi-circular interface of radius $r = r_b$ centered at x_0.

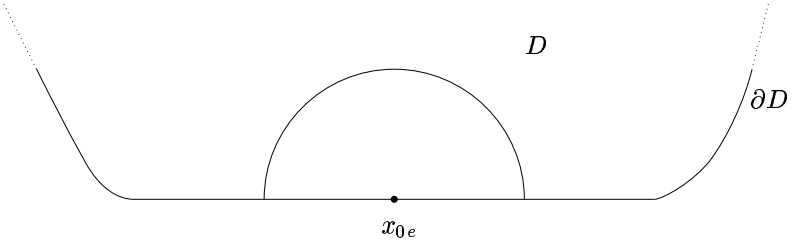

Figure 5: Plot of ∂D for which the center of the interface is at an unstable equilibrium. Here K_L, $K_R > 0$.

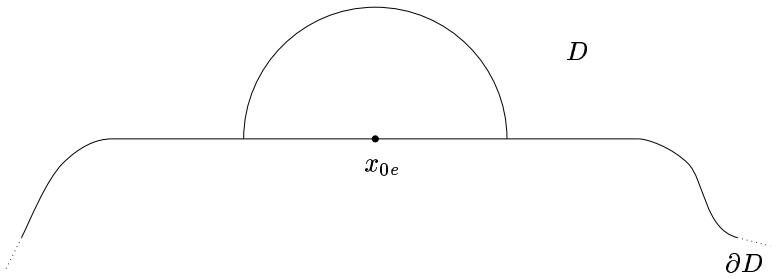

Figure 6: Plot of ∂D for which the center of the interface is at a stable steady state. Here K_L, $K_R < 0$.

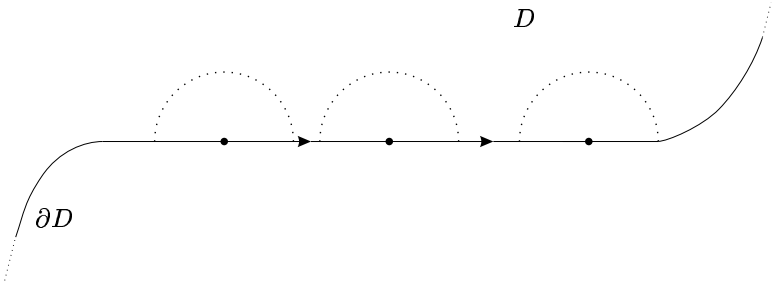

Figure 7: Plot of ∂D for which the center of the interface moves toward the right. Here $K_L < 0$ and $K_R > 0$.